Increasing functional avidity of TCR-redirected T cells by removing defined *N*-glycosylation sites in the TCR constant domain

Jürgen Kuball,[1,3,5] Beate Hauptrock,[6] Victoria Malina,[5] Edite Antunes,[5] Ralf-Holger Voss,[6] Matthias Wolfl,[1,3] Roland Strong,[2,4] Matthias Theobald,[5] and Philip D. Greenberg[1,3]

[1]Program in Immunology and [2]Basic Sciences Division, Fred Hutchinson Cancer Research Center, Seattle, WA 98109
[3]Department of Immunology and [4]Department of Immunology/Biochemistry, University of Washington School of Medicine, Seattle, WA 98195
[5]Department of Hematology and VanCreveld Clinic, Department of Immunology, University Medical Center Utrecht, 3584EA Utrecht, Netherlands
[6]Department of Hematology and Oncology, University of Mainz, 51101 Mainz, Germany

Adoptive transfer of T lymphocytes transduced with a T cell receptor (TCR) to impart tumor reactivity has been reported as a potential strategy to redirect immune responses to target cancer cells (Schumacher, T.N. 2002. *Nat. Rev. Immunol.* 2:512–519). However, the affinity of most TCRs specific for shared tumor antigens that can be isolated is usually low. Thus, strategies to increase the affinity of TCRs or the functional avidity of TCR-transduced T cells might be therapeutically beneficial. Because glycosylation affects the flexibility, movement, and interactions of surface molecules, we tested if selectively removing conserved *N*-glycoslyation sites in the constant regions of TCR α or β chains could increase the functional avidity of T cells transduced with such modified TCRs. We observed enhanced functional avidity and improved recognition of tumor cells by T cells harboring TCR chains with reduced *N*-glycosylation (ΔTCR) as compared with T cells with wild-type (WT) TCR chains. T cells transduced with WT or ΔTCR chains bound tetramer equivalently at 4°C, but tetramer binding was enhanced at 37°C, predominantly as a result of reduced tetramer dissociation. This suggested a temperature-dependent mechanism such as TCR movement in the cell surface or structural changes of the TCR allowing improved multimerization. This strategy was effective with mouse and human TCRs specific for different antigens and, thus, should be readily translated to TCRs with any specificity.

CORRESPONDENCE
Jürgen Kuball:
j.h.e.kuball@umcutrecht.nl
OR
Philip D. Greenberg:
pgreen@u.washington.edu

Abbreviations used: ΔTCR, TCR chains with reduced *N*-glycosylation; HLA-A2, HLA-A*0201; MFI, mean fluorescence intensity; N-X-S/T, asparagine–any amino acid–serine/threonine; NOD, non-obese diabetic; pMHC, peptide–MHC; SCID, severe combined immunodeficiency.

The transfer of defined TCR genes into human T cells appears to be a promising new strategy for redirecting T cells against cancer cells. In this approach, TCR genes with specificity for a known tumor antigen are introduced into the T cells of a patient whose tumor expresses the antigen and shares the MHC-restricting allele, and the modified cells are then expanded in vitro and infused back into the patient (1). A recent clinical study demonstrated the feasibility of this strategy (2), but the observed clinical efficacy was limited, in part because of the low avidity of the transduced T cells. Thus, a major challenge is to define means to improve the avidity of T cells transduced with a potentially tumor-reactive TCR, particularly in the context of the generally low affinity of available tumor-reactive TCRs. Besides selecting tumor-reactive TCRs with the highest identifiable affinity (3–5), strategies to increase TCR affinity before transduction (6, 7) or the (functional) avidity of the resulting TCR-transduced T cells (8, 9) should be explored. In this context, "affinity" will be defined as the strength of binding of one receptor with its ligand, "avidity" as the strength of binding between multiple

The Rockefeller University Press $30.00
J. Exp. Med. Vol. 206 No. 2 463-475
www.jem.org/cgi/doi/10.1084/jem.20082487

The Journal of Experimental Medicine

receptors and their ligands, and "functional avidity" as the sensitivity of a T cell response to a target cell expressing the relevant peptide–MHCs (pMHCs).

Different strategies have been examined to increase the affinity of TCRs used for transduction. TCR phage (7) and yeast (6) displays have been used as formats to express TCR chains and to then generate mutants that can be screened ex vivo for increased affinity. With these approaches, a library of TCR chains can be created generally after random mutation of defined regions, such as CDR3, known to be important in recognition; the library expressed on the surface of the phage or yeast; the expressed mutated TCR chains screened by tetramer binding for increased affinity; and the cDNA encoding the highest affinity chains extracted, characterized, and subsequently used for transduction. Consequently, these display strategies can be very effective but are cumbersome and must be individualized for each TCR. Furthermore, not every TCR can be successfully expressed and modified by these technically challenging display strategies in nonmammalian systems (unpublished data), emphasizing the need for alternative techniques to increase TCR affinity or functional avidity of a T cell.

The functional avidity of a T cell, as reflected by responsiveness to antigen, is modulated by T cell surface *O*- or *N*-glycosylation (10, 11), with increased glycosylation of T cell surface proteins associated with an increased activation threshold. This has been reported to contribute to the higher activation thresholds of tolerant T cells (12), aged as compared with young T cells (13, 14), and naive as compared with activated or memory T cells (15, 16), and molecules such as CD43 and CD45 have been reported to be directly involved. The reciprocal event, decreased glycosylation of surface proteins, has been reported to result in a decreased activation threshold. For example, decreased glycosylation of CD8 during thymic development is associated with increased affinity of CD8 with pMHC and, subsequently, improved signaling (17, 18). Moreover, a general deficiency in β1,6 *N*-acetylglucosaminyltransferase V (Mgat5) in mice, an enzyme in the *N*-glycosylation pathway, mediates increased T cell activity in vitro and results in autoimmune disease in vivo (19). Although deficiency of this *N*-glycosylation pathway enzyme in mice resulted in reduced *N*-glycosylation of all proteins, the reduced *N*-glycosylation of the TCRs appeared to specifically result in increased TCR mobility at the cell surface, enhanced recruitment to the synapse (TCR clustering), improved TCR engagement/down-modulation, and, consequently, enhanced functional avidity of the T cells. To test if selectively reducing *N*-glycosylation of TCR chains might achieve some of these effects, *N*-glycosylation of cloned TCR genes was prevented by sequentially deleting before expression *N*-glycosylation motifs (asparagine–any amino acid–serine/threonine[N-X-S/T]) in the α and/or β chain by changing N to glutamine (Q) by site-directed mutagenesis. The WT and/or modified TCR chains were expressed in hybridomas or human T cells, and TCR expression, tetramer staining, and functional avidity of the T cells was assessed. We demonstrate with several TCRs recognizing different antigens that the removal by point mutation of defined *N*-glycosylation motifs in the constant domains of TCR chains can increase the functional avidity of T cells transduced with these TCRs, and that this translates into enhanced recognition of tumor cells. As these *N*-glycosylation sites in the constant domain are conserved in all TCRs, this strategy should be easily translated to TCRs with any specificity.

RESULTS

Selective *N*-deglycosylation of TCR chains increases functional avidity of TCR-transduced 58α⁻β⁻ cells as compared with 58α⁻β⁻ cells transduced with WT TCR chains

To determine if reducing *N*-glycosylation of TCR chains can affect functional T cell avidity, we first analyzed the α and β chain sequence of two mouse (3, 4) and one human (9) TCRs for characteristic *N*-glycosylation sites (N-X-S/T; see Materials and methods; Fig. 1), as located according to the ImMunoGeneTics (IMGT) nomenclature (20). *N*-glycosylation sites were detected in the variable domain of all analyzed α chains but not in the variable domain of any of the tested β chains (Fig. 1). The mouse constant α chain harbors two *N*-glycosylation sites (c-90 and c-113). Although the location of these *N*-glycosylation sites are conserved in the human constant α chain (c-90 and c-109), the threonine of the motifs is replaced by an equally acceptable serine residue. The human constant α chain also has an additional *N*-glycosylation site at position c-36. The mouse constant β chain has three *N*-glycosylation sites, whereas the human constant β chain harbors only a single

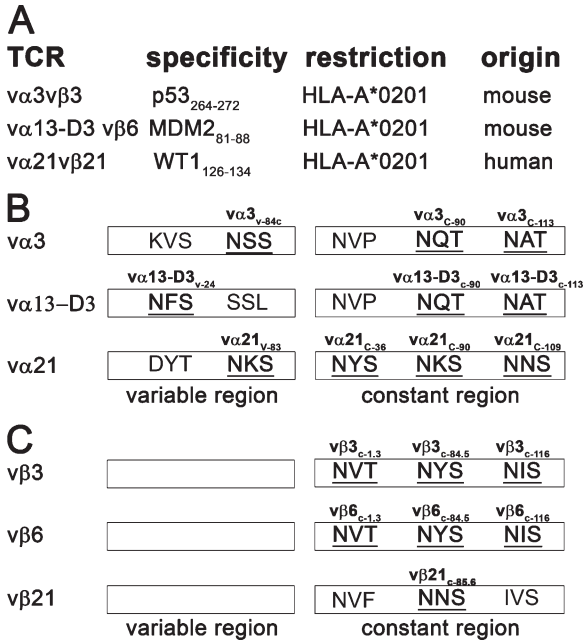

Figure 1. *N*-glycosylation sites in mouse and human TCR chains. (A) List of the cloned TCR chains investigated. *N*-glycosylation sites in these (B) TCR α and (C) TCR β chains. Sites harboring the *N*-glycosylation motif (N-X-S/T) are in bold and are underlined (according to the IMGT nomenclature; reference 20).

N-glycosylation site at position c-85.6, which corresponds to the mouse *N*-glycosylation site at position c-84.5.

The potential contribution of distinct glycosylation sites within TCR chains to modulating activation after antigen encounter was assessed by modifying WT mouse $v\alpha3_{WT}$ and $v\beta3_{WT}$TCR chains isolated from a mouse $CD8^+$ T cell clone that had been derived from a transgenic mouse expressing human HLA-A*0201 (HLA-A2) and was specific for the HLA-A2–restricted p53-derived epitope $p53_{264\text{-}272}$ (4). Furthermore, this TCR is CD8 independent, thus allowing analysis of the role of CD8 in the function of a deglycosylated TCR chain. *N*-glycosylation of TCR chains was prevented at specific sites (TCR chains with reduced *N*-glycosylation [ΔTCR]) by mutating N of the *N*-glycosylation motif N-X-S/T to Q at position 84C ($v\alpha3_{v\text{-}84C}$) in the variable domain of vα3 or at position 90 ($v\alpha3_{c\text{-}90}$) or 113 ($v\alpha3_{c\text{-}113}$) in the constant domain of the α chain, or at position 1.3 ($v\beta3_{c\text{-}1.3}$), 84.5 ($v\beta3_{c\text{-}84.5}$), or 116 ($v\beta3_{c\text{-}116}$) in the constant domain of the vβ3 chain ($v\beta3_{116}$; residues noted according to IMGT [20]; Fig. 1). $58\alpha^-\beta^-$ thymoma cells were retrovirally transduced with either the WT α and β chain or a combination of a WT chain and the corresponding Δα or Δβ TCR chain, selected with antibiotics, stained with an antibody to the mouse β TCR chain, and analyzed by flow cytometry. Only $58\alpha^-\beta^-$ cells transduced with both vα3 and vβ3 chains expressed the vβ3 chain at the cell surface (unpublished data), consistent with the requirement for the assembly of paired heterodimeric TCR chains to achieve surface expression. Despite multiple attempts, we were unable to generate $58\alpha^-\beta^-$ cells expressing the $v\beta3_{c\text{-}1.3}$ chain, perhaps because of improper folding of this modified chain, and this modification was therefore not further pursued. After transduction of $58\alpha^-\beta^-$ cells with WT $v\alpha3_{WT}/v\beta3_{WT}$ chains or all other combinations of Δ and WT TCR chains, ∼80% of cells expressed the vβ3 TCR, with a mean fluorescence intensity (MFI) of ∼250 for vβ3 expression (Fig. 2 A; and Fig. S1, available at http://www.jem.org/cgi/content/full/jem.20082487/DC1). Because the α chain is required for surface expression of the β chain, these results also suggest that the mutations do not affect expression, with equivalent amounts of Δ and WT vα3 chains expressed at the cell surface with vβ3 chains. Thus, $58\alpha^-\beta^-$ cells transduced with combinations of Δ and WT chains exhibited similar efficiencies of expression for pairs of all of the introduced αβ TCR chains, with the exception of the $v\beta3_{c\text{-}1.3}$ chain.

To assess tetramer binding of the different TCR chains, $58\alpha^-\beta^-$ cells mock transduced or transduced with WT only or combinations of WT and ΔTCR chains were incubated with the $p53_{264\text{-}272}$ tetramer at 4°C for analysis by flow cytometry of TCR–pMHC interactions in the absence of temperature-dependent mechanisms such as increased membrane fluidity, diffusion rates, and conformational changes. Mock-transduced $58\alpha^-\beta^-$ cells did not bind the $p53_{264\text{-}272}$ tetramer. In contrast, ∼70% of the $58\alpha^-\beta^-$ cells transduced with any of the pairs of TCR chains bound the $p53_{264\text{-}272}$ tetramer, and the MFI of the tetramer-positive populations was ∼40–70 for $58\alpha^-\beta^-$ cells expressing WT and ΔTCR chains (Fig. 2 B; and Fig. S2, available at http://www.jem.org/cgi/content/full/jem.20082487/DC1). Thus, $58\alpha^-\beta^-$ cells transduced with combinations of ΔTCR chains exhibited similar levels of TCR expression as compared with $58\alpha^-\beta^-$ cells transduced with WT TCR chains and exhibited no initial difference in specific tetramer binding.

To assess functional avidity of transduced $58\alpha^-\beta^-$ cells, IL-2 secretion was assessed in response to K562-A2 cells pulsed with titrated amounts of $p53_{264\text{-}272}$ peptide. The peptide concentration required to reach half-maximal IL-2 secretion (EC50) was calculated and transformed to log scale ($\log_{EC50}$). $58\alpha^-\beta^-$ cells expressing $v\alpha3_{WT}/v\beta3_{WT}$ TCR had a $\log_{EC50}$ of -6 ± 0.1 M, and $58\alpha^-\beta^-$ cells expressing $v\alpha3_{c\text{-}90}/v\beta3_{WT}$ had

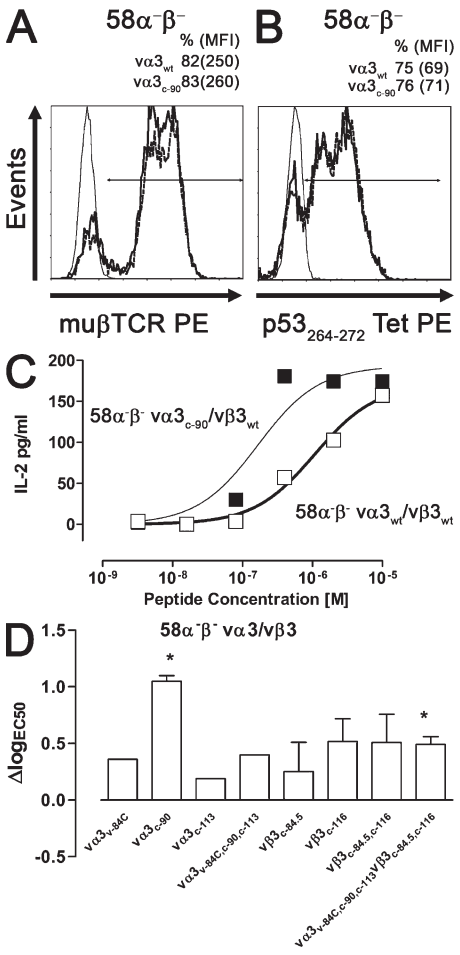

Figure 2. Analysis of the vα3vβ3 TCR–transduced hybridoma cell line $58\alpha^-\beta^-$. Mock (thin line), $v\alpha3_{WT}/v\beta3_{WT}$ (bold line), and $v\alpha3_{c\text{-}90}/v\beta3_{WT}$ (dashed line) TCR–transduced $58\alpha^-\beta^-$ cells were stained with (A) anti-muβTCR-PE or (B) $p53_{264\text{-}272}$Tet-PE at 4°C and were analyzed by flow cytometry. (C) $v\alpha3_{WT}/v\beta3_{WT}$ (□) and $v\alpha3_{c\text{-}90}/v\beta3_{WT}$ (■) TCR–transduced $58\alpha^-\beta^-$ cells were co-cultured with K562-A2 targets pulsed with titrated amounts of $p53_{264\text{-}272}$ peptide, and IL-2 secretion was measured by ELISA. Data are representative of at least two independent experiments. (D) $\Delta\log_{EC50}$ of ΔTCR-transduced T cells as compared with WT TCR–transduced T cells was determined as $\log_{EC50\Delta} - \log_{EC50WT}$. Statistical significance was assessed by a *t* test (*, $P < 0.05$; error bars are SEM) if two or more independent cytokine titration assays were available for the calculation of $\Delta\log_{EC50}$.

a $\log_{EC50}$ of –6.9 ± 0.3 M (Fig. 2 C), revealing a 0.9-log increased avidity for the $v\alpha3_{c\text{-}90}/v\beta3_{WT}$– compared with WT TCR–transduced cells ($\Delta\log_{EC50}$ $v\alpha3_{c\text{-}90}$ = 0.9; Fig. 2 D). IL-2 secretion in response to peptide-loaded K562-A2 cells was also measured for $58\alpha^-\beta^-$ cells transduced with the other mutants (not depicted), and the $\Delta\log_{EC50}$ was calculated ($v\alpha3_{v\text{-}84C}$, 0.4; $v\alpha3_{c\text{-}113}$, 0.2; $v\alpha3_{v\text{-}84C,c\text{-}90,c\text{-}113}$, 0.5; $v\beta3_{c\text{-}84.5}$, 0.3; $v\beta3_{c\text{-}116}$, 0.5; $v\beta3_{c\text{-}84.5,c\text{-}116}$, 0.5; and $v\alpha3_{v\text{-}84C,c\text{-}90,c\text{-}113}/v\beta3_{c\text{-}84.5,c\text{-}116}$, 0.5; Fig. 2 D). *t* tests were performed if two or more independent cytokine titration assays were available for the calculation of $\Delta\log_{EC50}$ to determine the significance of the observed improvement in functional avidity ($v\alpha3_{c\text{-}90}$, P = 0.01; $v\beta3_{c\text{-}84.5}$, P = 0.44; $v\beta3_{c\text{-}116}$, P = 0.06; $v\beta3_{c\text{-}84.5,c\text{-}116}$, P = 0.07; $v\alpha3_{v\text{-}84C,c\text{-}90,c\text{-}113}/v\beta3_{c\text{-}84.5,c\text{-}116}$, P = 0.02; Fig. 2 D). In summary, despite equivalent TCR expression and equivalent binding at 4°C of specific tetramer by $58\alpha^-\beta^-$ cells transduced with WT and ΔTCR, reduced *N*-glycosylation of TCR chains increased IL-2 secretion of $58\alpha^-\beta^-$ cells after antigen encounter, and was statistically significant (P < 0.05) for $58\alpha^-\beta^-$ cells transduced with $v\alpha3_{c\text{-}90}$ and $v\alpha3_{v\text{-}84C,c\text{-}90,c\text{-}113}/v\beta3_{c\text{-}84.5,c\text{-}116}$ chains.

Enhanced functional avidity of human T cells transduced with the partially deglycosylated TCR chain $v\alpha3_{c\text{-}90}$ in the absence of the CD8 coreceptor

To determine if the effect of partial TCR chain deglycosylation in human T cells reflected altered interactions with the CD8 coreceptor, human $CD4^+$ and $CD8^+$ T cells were retrovirally transduced with the HLA-A2–restricted $p53_{264\text{-}272}$–specific mouse WT or ΔTCR, as indicated in Materials and methods. We focused our analysis on the $v\alpha3_{c\text{-}90}/v\beta3_{WT}$ ΔTCR chain pair that had the most prominent change in avidity in $58\alpha^-\beta^-$ cells. $CD4^+$ T cells expressing mouse $v\alpha3_{WT}/v\beta3_{WT}$ or $v\alpha3_{c\text{-}90}/v\beta3_{WT}$ TCR chains were sorted for equivalent amounts of vβ3 surface expression and were expanded (both were 99% vβ3 positive; $v\alpha3_{WT}/v\beta3_{WT}$, MFI of 1,050; $v\alpha3_{c\text{-}90}/v\beta3_{WT}$, MFI of 1,100; Fig. 3 A). Expression of the vα3 chain could not be monitored directly because of the lack of a commercially available antibody. However, mouse TCR chains are preferentially expressed with each other and not with human endogenous TCR chains (8, 21, 22), and measuring the introduced β chain should be a good general indication of expression of the introduced mouse α chain in these polyclonal populations. Moreover, vα3 expression was indirectly assessed by isolating mRNA from the transduced T cells, reverse transcribing the mRNA into cDNA, analyzing the product with PCR primers detecting the unique CDR3 domain of the TCR α chain, and normalizing to the number of β-actin copies. Equivalent amounts (1:1 ratio) of $v\alpha3_{WT}$ and $v\alpha3_{c\text{-}90}$ RNA levels were detected in cells previously selected based on equivalent vβ3 surface expression.

To assess tetramer binding of WT and ΔTCR chain heterodimers in human T cells in the absence of the CD8 coreceptor, transduced $CD4^+$ T cells were incubated with $p53_{264\text{-}272}$ tetramer at 4°C and analyzed by flow cytometry. Tetramer binding of $CD4^+$ T cells transduced with $v\alpha3_{WT}/v\beta3_{WT}$ and $v\alpha3_{c\text{-}90}/v\beta3_{WT}$ TCR chains was almost equivalent (both 97% tetramer positive; $v\alpha3_{WT}/v\beta3_{WT}$, MFI of 66; $v\alpha3_{c\text{-}90}/v\beta3_{WT}$, MFI of 57; Fig. 3 B). Functional avidity of the $CD4^+$ T cells transduced with $v\alpha3_{WT}/v\beta3_{WT}$ and $v\alpha3_{c\text{-}90}/v\beta3_{WT}$ TCR chains was then determined by incubating the T cells with T2 cells pulsed with titrated amounts of $p53_{264\text{-}272}$ peptide. Supernatant was harvested 48 h later, IFN-γ secretion was determined by ELISA, and the peptide

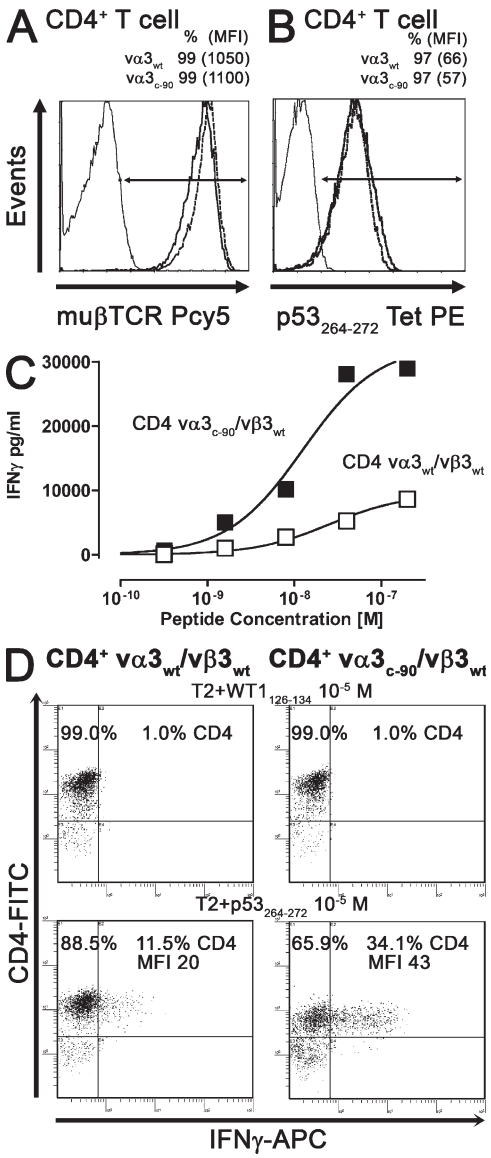

Figure 3. Analysis of vα3vβ3 TCR–transduced $CD4^+$ T cells. Mock (thin line), $v\alpha3_{WT}/v\beta3_{WT}$ (bold line), and $v\alpha3_{c\text{-}90}/v\beta3_{WT}$ (dashed line) TCR–transduced $CD4^+$ T cells were stained with (A) anti-muβTCR–Pcy5 or (B) $p53_{264\text{-}272}$Tet–PE at 4°C and were analyzed by flow cytometry. (C) $v\alpha3_{WT}/v\beta3_{WT}$ (□) and $v\alpha3_{c\text{-}90}/v\beta3_{WT}$ (■) TCR–transduced $CD4^+$ T cells were co-cultured with T2 cells pulsed with titrated amounts of $p53_{264\text{-}272}$ peptide. IFN-γ secretion was measured by ELISA after 48 h. (D) Intracellular IFN-γ secretion of $v\alpha3_{WT}/v\beta3_{WT}$ and $v\alpha3_{c\text{-}90}/v\beta3_{WT}$ TCR–transduced $CD4^+$ T cells was determined after a 5-h coincubation with T2 cells pulsed with 10^{-5} M $WT1_{126\text{-}134}$ or $p53_{264\text{-}272}$ peptide. Data are representative of at least two independent experiments.

concentration inducing half-maximal IFN-γ secretion was determined and transformed to $\log_{EC50}$. The $v\alpha3_{WT}/v\beta3_{WT}$–transduced T cells had a $\log_{EC50}$ for IFN-γ secretion of −7.5 ±0.1 M (Fig. 3 C), whereas the $V\alpha3_{c\text{-}90}/v\beta3_{WT}$ TCR–transduced $CD4^+$ T cells had a $\log_{EC50}$ of −7.9 ± 0.1 M (Fig. 3 C). Again, $\Delta\log_{EC50}$ (0.4) was calculated from two independent assays ($P = 0.02$). Furthermore, as compared with WT TCR–transduced $CD4^+$ T cells, the maximal IFN-γ cytokine secretion was approximately threefold higher for $CD4^+$ T cells transduced with $v\alpha3_{c\text{-}90}/v\beta3_{WT}$ TCR chains ($v\alpha3_{WT}/v\beta3_{WT}$, 3,258 ± 1,638 pg/ml; $v\alpha3_{c\text{-}90}/v\beta3_{WT}$, 9,487 ± 382 pg/ml). Thus, despite equivalent amounts of TCR surface expression and tetramer binding by the transduced $CD4^+$ T cells, $CD4^+$ T cells transduced with $v\alpha3_{c\text{-}90}/v\beta3_{WT}$ TCR chains had a greater ability to respond to antigen and produce IFN-γ than $CD4^+$ T cells expressing $v\alpha3_{WT}/v\beta3_{WT}$ chains.

To determine if the observed higher maximal IFN-γ cytokine secretion by $v\alpha3_{c\text{-}90}/v\beta3_{WT}$ compared with $v\alpha3_{WT}/v\beta3_{WT}$ TCR–transduced T cells reflected recruitment of a larger fraction of antigen-specific cells, or more cytokine production from each activated cell, transduced T cells were incubated for 5 h with $p53_{264\text{-}272}$ or $WT1_{126\text{-}134}$ control peptide-pulsed (10^{-5} M) target cells, secretion was blocked with Brefeldin A, and intracellular IFN-γ production was determined by flow cytometry. 11.5% of $CD4^+$ T cells transduced with $v\alpha3_{WT}/v\beta3_{WT}$ and 34.1% of $CD4^+$ T cells transduced with $v\alpha3_{c\text{-}90}/v\beta3_{WT}$ stained positive for IFN-γ (Fig. 3 D). Furthermore, the MFI of IFN-γ–positive cells, an indicator for the mean cytokine production per cell, was 20 for $v\alpha3_{WT}/v\beta3_{WT}$– and 43 for $v\alpha3_{c\text{-}90}/v\beta3_{WT}$–transduced T cells, suggesting that the difference reflected both recruitment of more cells and production of more cytokine per cell in cells expressing the $v\alpha3_{c\text{-}90}/v\beta3_{WT}$ TCR.

Gain of functional avidity mediated by the $v\alpha3_{c\text{-}90}$ TCR chain persists in the presence of the CD8 coreceptor

To determine if the presence of the $CD8^+$ coreceptor modifies the observed improvement in functional avidity with ΔTCR chains, $CD8^+$ T cells transduced with either $v\alpha3_{WT}/v\beta3_{WT}$ or $v\alpha3_{c\text{-}90}/v\beta3_{WT}$ were selected for equivalent vβ3 TCR surface expression. To determine α chain expression in cells sorted for equivalent vβ3 TCR surface expression, mRNA was again isolated from transduced T cells, reverse transcribed into cDNA, amplified by PCR with primers specific for the TCR α chain and β-actin, and normalized to β-actin copies. Equivalent amounts (1:1 ratio) of $v\alpha3_{WT}$ and $v\alpha3_{c\text{-}90}$ RNA were detected. Transduced $CD8^+$ T cells selected for equivalent vβ3 TCR surface expression by flow cytometry and controlled for equivalent vα3 TCR expression by RT-PCR were incubated for 5 h with $p53_{264\text{-}272}$ or $WT1_{126\text{-}134}$ control peptide-pulsed (10^{-5} M) T2 cells, secretion was blocked with Brefeldin A, and intracellular IFN-γ production was determined by flow cytometry. 42.5% of $v\alpha3_{c\text{-}90}/v\beta3_{WT}$–transduced $CD8^+$ T cells produced IFN-γ (MFI of 40), whereas only 27.7% of cells expressing $v\alpha3_{WT}/v\beta3_{WT}$ produced IFN-γ (MFI of 29; Fig. 4 A). Thus, although the presence of the coreceptor CD8 increased the functional avidity of this class I–restricted T cell response, recruitment of T cells and production of cytokine per cell was still further increased in the presence of ΔTCR as compared with WT TCR chains.

To assess the impact of a ΔTCR in transduced T cells on recognition of cells expressing more physiological levels of antigen, mock-transduced T cells and $v\alpha3_{c\text{-}90}/v\beta3_{WT}$ or $v\alpha3_{WT}/v\beta3_{WT}$ TCR–transduced $CD8^+$ T cells were tested for recognition of the HLA-A2–positive p53-negative cell line Soas2, and the HLA-A2–positive p53-overexpressing tumor cell lines MDAMB231, SW480, and MZ1851RC in a 5-h ^{51}Cr-release assay at a low effector/target ratio of 0.3:1 (Fig. 4 B). No T cell lines lysed the negative control Saos2, and mock-transduced T cells did not lyse any tumor targets. In contrast, the

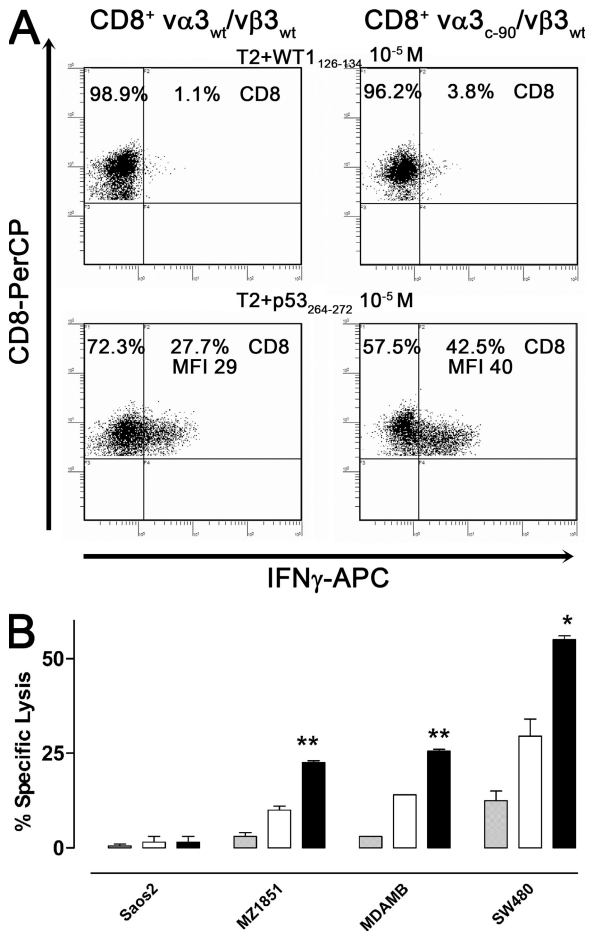

Figure 4. Analysis of vα3vβ3 TCR–transduced $CD8^+$ T cells. (A) Intracellular IFN-γ secretion of $v\alpha3_{WT}/v\beta3_{WT}$ and $v\alpha3_{c\text{-}90}/v\beta3_{WT}$ TCR–transduced $CD8^+$ T cells was determined after a 5-h coincubation with T2 cells pulsed with 10^{-5} M $WT1_{126\text{-}134}$ or $p53_{264\text{-}272}$ peptide. (B) Mock (gray bar), $v\alpha3_{WT}/v\beta3_{WT}$ (white bar), and $v\alpha3_{c\text{-}90}/v\beta3_{WT}$ (black bar) TCR–transduced $CD8^+$ T cells were tested for recognition of the HLA-$A2^+p53^-$ cell line Saos2 and the p53-overexpressing cell lines MDAMB231 (MDAMB), SW480, and MZ1851RC (MZ1851) in a 5-h ^{51}Cr-release assay (*t* test: *, $P < 0.05$; **, $P < 0.01$; error bars are SEM). All assays were performed in duplicates. All data are representative of at least two independent experiments.

$v\alpha3_{c\text{-}90}/v\beta3_{WT}$ and $v\alpha3_{WT}/v\beta3_{WT}$ TCR–transduced $CD8^+$ T cells lysed all of the p53-overexpressing cell lines. Greater lysis of tumor targets was achieved with T cells transduced with the ΔTCR chains, which was significantly different by a *t* test from lysis by T cells transduced with WT TCR chains (ΔTCR/WT TCR: MZ1851RC, 23%/11%, $P < 0.01$; MDAMB231, 26%/14%, $P < 0.01$; SW480, 55%/30%, $P < 0.05$). Thus, substituting $v\alpha3_{WT}$ with $v\alpha3_{c\text{-}90}$ improved lysis of cells that endogenously process and present antigen.

Tetramer binding of T cells transduced with WT and partially deglycosylated TCR chains

Functional avidity of TCR-transduced T cells has been reported to correlate with tetramer binding (9). However, our results with transduced $58\alpha^-\beta^-$, $CD4^+$, and $CD8^+$ T cells indicated an increase in functional avidity for $v\alpha3_{c\text{-}90}/v\beta3_{WT}$– compared with $v\alpha3_{WT}/v\beta3_{WT}$–transduced cells despite apparently equivalent tetramer binding (Figs. 2–4). Because these tetramer-binding experiments were performed at 4°C, which precludes temperature-dependent events such as increased membrane fluidity and conformational changes, tetramer binding was reanalyzed at 37°C to permit temperature-dependent changes that might influence TCR–pMHC binding (23–25), and the K_D of the TCR-pMHC interaction was calculated by Scatchard analysis, as indicated in Materials and methods. The $v\alpha3_{WT}/v\beta3_{WT}$ and $v\alpha3_{c\text{-}90}/v\beta3_{WT}$ TCR–transduced $CD4^+$ T cells had a K_D of 73 and 46 nM, respectively, and the $v\alpha3_{WT}/v\beta3_{WT}$ and $v\alpha3_{c\text{-}90}/v\beta3_{WT}$ TCR–transduced $CD8^+$ T cells had a K_D of 19 and 15 nM, respectively (Table I and Fig. 5, A and B). Thus, in contrast to tetramer binding at 4°C, analysis at 37°C revealed that the $v\alpha3_{c\text{-}90}/v\beta3_{WT}$ TCR–transduced $CD4^+$ T cells bound tetramer with a lower K_D than WT receptors, whereas $CD8^+$ T cells transduced with the $v\alpha3_{c\text{-}90}/v\beta3_{WT}$ TCR appeared to achieve only a slightly improved K_D compared with WT TCR–transduced T cells. To more precisely analyze the K_D changes in $CD4^+$ and $CD8^+$ T cells, the K_D was reanalyzed by determining tetramer association and dissociation rather than the previous Scatchard analysis, which permitted determining the association (k_{on}) and dissociation (k_{off}) rates. As described in Materials and methods, k_{ob} was assessed during tetramer association; $t_{1/2}$ and k_{off} were assessed during tetramer dissociation; and k_{on} and K_D were then derived (Table I and Fig. 5, C–F). k_{off}, the dissociation constant of the pMHC from the TCR, was approximately ninefold longer for $CD8^+$ and approximately fourfold longer for $CD4^+$ΔTCR as compared with WT TCRs ($CD8^+v\alpha3_{c\text{-}90}/v\beta3_{WT}$, 0.26 min^{-1}; $CD8^+v\alpha3_{WT}/v\beta3_{WT}$, 0.03 min^{-1}; $CD4^+v\alpha3_{c\text{-}90}/v\beta3_{WT}$ TCR, 0.29 min^{-1}; and $CD4^+v\alpha3_{WT}/v\beta3_{WT}$, 0.07 min^{-1}). k_{on}, the association constant of the TCR to the pMHC complex for both WT and ΔTCR–transduced $CD8^+$ T cells, was 0.01 $nM^{-1}min^{-1}$, 0.0007 $nM^{-1}min^{-1}$, and ≤0.0007 $nM^{-1}min^{-1}$ for Δ and WT TCR $CD4^+$ T cells. These more precise rates now resulted in a lower calculated K_D for ΔTCR-transduced $CD8^+$ and $CD4^+$ T cells ($CD8^+v\alpha3_{c\text{-}90}/v\beta3_{WT}$ TCR, 3 nM; $CD8^+v\alpha3_{WT}/v\beta3_{WT}$, 26 nM; $CD4^+v\alpha3_{c\text{-}90}/v\beta3_{WT}$ TCR, 100 nM; and $CD4^+v\alpha3_{WT}/v\beta3_{WT}$, ≥414 nM), consistent with the higher functional avidity previously observed for ΔTCR as compared with WT TCR–transduced T cells.

TCR internalization of WT and ΔTCR in transduced T cells after antigen-specific stimulation

Globally reduced *N*-glycosylation in T cells has been suggested to improve T cell signaling by improving mobility of the TCR on the cell membrane, thereby enhancing TCR recruitment to the synapse and increasing the frequency of TCR–pMHC interaction, which results in augmented signaling and greater TCR internalization/endocytosis (19). We examined whether depletion of a single *N*-glycosylation

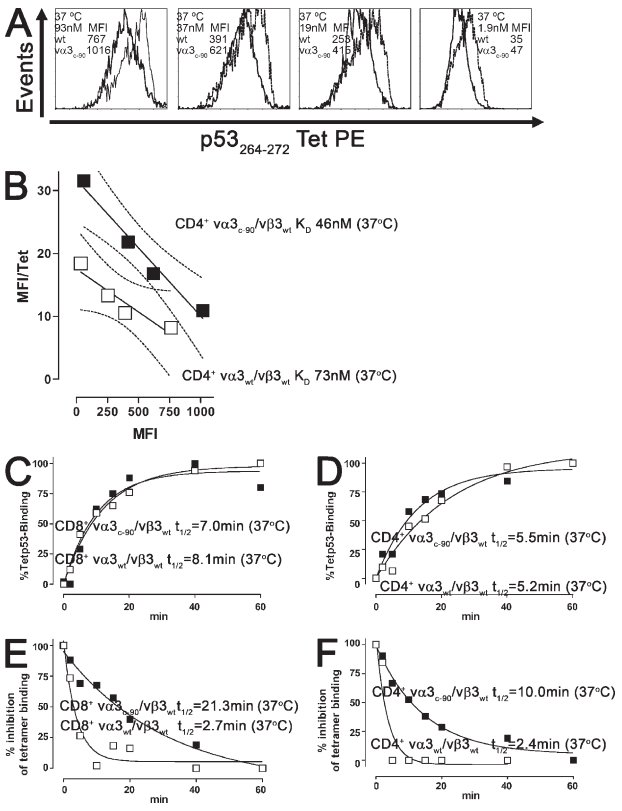

Figure 5. Tetramer binding of WT and ΔTCR–transduced T cells. (A) $v\alpha3_{WT}/v\beta3_{WT}$ (bold line) and $v\alpha3_{c\text{-}90}/v\beta3_{WT}$ (dashed line) TCR–transduced $CD4^+$ T cells were stained with $p53_{264\text{-}272}$Tet-PE at 37°C at the indicated tetramer concentrations. (B) $v\alpha3_{WT}/v\beta3_{WT}$ (□) and $v\alpha3_{c\text{-}90}/v\beta3_{WT}$ (■) TCR–transduced $CD4^+$ T cells were tested for binding to $p53_{264\text{-}272}$Tet-PE after 60 min by flow cytometry as indicated in A, and the avidity (K_D) of tetramer binding to T cells was determined by Scatchard analysis, with the 95% confidence band indicated by thin dashed lines. $p53_{264\text{-}272}$Tet-PE binding to $v\alpha3_{WT}/v\beta3_{WT}$ (□) and $v\alpha3_{c\text{-}90}/v\beta3_{WT}$ (■) TCR–transduced (C) $CD8^+$ and (D) $CD4^+$ T cells was determined at 37°C at the indicated time points by flow cytometry, and $t_{1/2}$ for half maximal binding was determined. After $p53_{264\text{-}272}$Tet-PE binding to $v\alpha3_{WT}/v\beta3_{WT}$ (□) and $v\alpha3_{c\text{-}90}/v\beta3_{WT}$ (■) TCR–transduced (E) $CD8^+$ and (F) $CD4^+$ T cells, the cells were washed and incubated with the HLA class I blocking antibody W6/32 at 37°C. The percent inhibition of tetramer binding and $t_{1/2}$ for inhibition were calculated. All data are representative of at least two independent experiments.

motif from a TCR chain can also facilitate this process, and used TCR internalization as the measurable objective endpoint. Therefore, $v\alpha3_{c\text{-}90}/v\beta3_{WT}$ or $v\alpha3_{WT}/v\beta3_{WT}$ TCR–transduced $CD4^+$ T cells were co-cultured with T2 cells pulsed with 10^{-6} or 10^{-8} M of $p53_{264\text{-}272}$ peptide, and surface expression of the introduced TCR β chain was assessed before and at 2, 4, and 6 h after stimulation by flow cytometry. For the comparisons, surface expression of the introduced mouse TCR β chain before antigen encounter was set as 100%, no detectable surface expression of mouse TCR β chain was set as 0%, and the surface expression after antigen encounter was calculated as the percentage of total TCR β chain surface expression before antigen encounter. A maximal 80% down-regulation of the introduced mouse TCR β chain was observed at 10^{-6} M, and 50% TCR β chain down-regulation was observed at 10^{-8} M for both $v\alpha3_{c\text{-}90}/v\beta3_{WT}$ and $v\alpha3_{WT}/v\beta3_{WT}$ TCR–transduced $CD4^+$ T cells (Fig. S3, available at http://www.jem.org/cgi/content/full/jem.20082487/DC1). Thus, Δ and WT TCR chains were equivalently internalized after antigen encounter.

Depleting *N*-glycosylation motifs in the constant domain improves functional avidity of TCR with other specificities in transduced T cells

The enhanced avidity of $v\alpha3_{c\text{-}90}/v\beta3_{WT}$ as compared with $v\alpha3_{WT}/v\beta3_{WT}$–transduced T cells could potentially be a unique feature of the $p53_{264\text{-}272}$–specific vα3/vβ3 TCR chains. To determine if elimination of *N*-glycosylation modifications could be of more general use to increase the avidity of T cells transduced with other TCRs, a mouse HLA-A2–restricted TCR with reactivity against the human tumor antigen $MDM2_{81\text{-}88}$ ($v\alpha13\text{-}D3_{WT}/v\beta6_{WT}$) was modified at the unique position v-24 in the variable domain ($v\alpha13\text{-}D3_{v\text{-}24}$) or at the positions previously found to be most effective in improving the functional avidity of T cells for the vα3/vβ3 TCR chains: c-90 in the constant domain of the α chain

Table I. Tetramer-binding avidity (K_D) of TCR-transduced human T lymphocytes

	K_D ($K_D = -1$/slope determined by Scatchard plot)	K_D (determined by Tet association and Tet dissociation)	Tet association		Tet dissociation (inhibition with W6/32)		k_{on} calculation
		$K_D = k_{off}/k_{on}$	$t_{1/2}$	k_{ob}	$t_{1/2}$	k_{off}	$k_{on} = (k_{ob} - k_{off})$/ ligand concentration
	nM	*nM*	*min*	min^{-1}	*min*	min^{-1}	$nM^{-1}min^{-1}$
$CD4^+$ $v\alpha3_{WT}$	73 (slope: −0.014 ± 0.003)	≥414	5.2 (95% CI interval: 2.4 to ∞)	0.13 ± 0.06	2.4 (95% CI interval: 1.1 to ∞)	0.29 ± 0.13	≤0.0007
$CD4^+$ $v\alpha3_{c\text{-}90}$	46 (slope: −0.032 ± 0.011)	100 ± 33	5.5 (95% CI interval: 3.2–18.9)	0.13 ± 0.04	10 (95% CI interval: 7.1–17.1)	0.07 ± 0.01	0.0007 ± 0.0001
$CD8^+$ $v\alpha3_{WT}$	19 (slope: −0.052 ± 0.003)	26 ± 7	8.1 (95% CI interval: 6.6–11.1)	0.85 ± 0.01	2.7 (95% CI interval: 1.6–9.3)	0.26 ± 0.07	0.01 ± 0.01
$CD8^+$ $v\alpha3_{c\text{-}90}$	15 (slope: −0.065 ± 0.008)	3 ± 1	7 (95% CI interval: 4.4–17.9)	0.99 ± 0.02	21.3 (95% CI interval: 12.5–72)	0.03 ± 0.01	0.01 ± 0.01
$CD8^+$ $v\alpha13\text{-}D3_{WT}$	14 (slope: −0.074 ± 0.026)	30 ± 3	8.3 (95% CI interval: 6.6–11.1)	0.08 ± 0.01	26.5 (95% CI interval: 7.8 to ∞)	0.03 ± 0.01	0.001 ± 0.001
$CD8^+$ $v\alpha13\text{-}D3_{c\text{-}90}$	12 (slope: −0.083 ± 0.043)	10 ± 1	7.1 (95% CI interval: 4.4–17.9)	0.1 ± 0.02	64 (95% CI interval: 10.8 to ∞)	0.01 ± 0.01	0.001 ± 0.001
$CD8^+$ $v\alpha21_{WT}$	n.d.	n.d.	n.d.	n.d.	n.d.	n.d.	n.d.
$CD8^+$ $v\alpha21_{c\text{-}36}$	n.d.	n.d.	n.d.	n.d.	n.d.	n.d.	n.d.

n.d., not determined because of the loss of tetramer binding at 37°C as compared with 0°C.

(vα13-D3$_{c\text{-}90}$) and c-116 in the constant domain of the β chain (vβ6$_{c\text{-}116}$; Fig. 1). CD8$^+$ T cells were retrovirally transduced with vectors encoding for WT or combinations of WT and ΔTCR chains. T cells transduced with each of these different pairs of chains exhibited equivalent amount of vβ6 chain at the cell surface (unpublished data). Transduced T cells were stimulated with K562-A2 cells pulsed with titrated amounts of MDM2$_{81\text{-}88}$ peptide, the number of IFN-γ–secreting cells was determined by an IFN-γ ELISPOT assay (unpublished data), and $\Delta\log_{EC50}$ was calculated for CD8$^+$-transduced T cells. The results (Fig. 6 A) revealed that removal of the *N*-glycoslyation site in the α chain at position c-90 significantly increased functional avidity (vα13-D3$_{c\text{-}90}$/vβ6$_{WT}$, $\Delta\log_{EC50}$ = 0.9 and P = 0.02). Removal of other *N*-glycosylation sites also appeared to increase functional avidity, but these changes did not reach statistical significance (vα13-D3$_{v\text{-}24}$/vβ6$_{WT}$, $\Delta\log_{EC50}$ = 0.3 and P = 0.55; vα13-D3$_{WT}$/vβ6$_{c\text{-}116}$, $\Delta\log_{EC50}$ = 0.8 and P = 0.07; and vα13-D3$_{c\text{-}90}$/vβ6$_{c\text{-}116}$, $\Delta\log_{EC50}$ = 0.3 and P = 0.15). As described with the tetramer binding of vα3/vβ3 TCR-transduced T cells, the K_D of vα13-D3$_{WT}$/vβ6$_{WT}$ and vα13-D3$_{c\text{-}90}$/vβ6$_{WT}$ was assessed by Scatchard analysis and by determining tetramer association and dissociation (Table I). As observed for vα3/vβ3 TCR–transduced T cells, the K_D was only slightly decreased for ΔTCR-transduced T cells when analyzed by Scatchard (vα13-D3$_{WT}$/vβ6$_{WT}$, 14 nM; vα13-D3$_{c\text{-}90}$/vβ6$_{WT}$, 12 nM). However, the more precise K_D calculation determined from the tetramer association and dissociation rates revealed an approximately threefold decrease in K_D for ΔTCR as compared with WT TCRs (vα13-D3$_{WT}$/vβ6$_{WT}$, 30 nM; vα13-D3$_{c\text{-}90}$/vβ6$_{WT}$, 10 nM), consistent with the higher functional avidity of ΔTCR- as compared with WT TCR–transduced T cells.

To determine if human TCR chains might also benefit from the removal of *N*-glycoslyation sites, human HLA-A2–restricted TCR chains (vα21$_{WT}$/vβ21$_{WT}$) specific for the tumor antigen epitope WT1$_{126\text{-}134}$ were modified at the unique position v-83 in the variable domain (vα21$_{v\text{-}83}$); positions c-36, c-90, and c-109 in the constant domain of the α chain (vα21$_{c\text{-}36}$, vα21$_{c\text{-}90}$, and vα21$_{c\text{-}109}$); or position c-85.6 in the β chain (vβ21$_{c\text{-}85.6}$). Human CD8$^+$ T cells were retrovirally transduced with vectors encoding WT or combinations of WT and ΔTCR chains and were selected for equivalent levels of vβ21 by flow cytometry (unpublished data). To formally assess vα21 expression, mRNA was isolated from transduced CD8$^+$ T cells, reverse transcribed into cDNA, and analyzed with PCR primers detecting the unique CDR3 domain of the TCR α chain and normalized to the number of β-actin copies. Equivalent amounts of WT and Δvα21 RNA were detected in cells previously selected based on equivalent vβ21 surface expression. Transduced CD8$^+$ T cells, controlled for equivalent amounts of introduced αβ TCR chains, were stimulated with T2 cells pulsed with WT1$_{126\text{-}134}$ peptide (10^{-5} M), and the number of IFN-γ–producing cells was determined by an intracellular cytokine secretion assay. Cells transduced with vα21$_{c\text{-}36}$/vβ6$_{WT}$ exhibited the greatest activity, with 20.6% of cells producing cytokine as compared with 6.1% for WT TCR–transduced T cells (Fig. 6 B). After transduction with vα21$_{v\text{-}83}$/vβ21$_{WT}$, vα21$_{c\text{-}90}$/vβ21$_{WT}$, vα21$_{c\text{-}109}$/vβ21$_{WT}$, or vα21$_{WT}$/vβ21$_{c\text{-}85.6}$, 4.9, 4.3, 8.3, and 8.6% of cells, respectively, produced IFN-γ (unpublished data). Because of the loss of tetramer binding at 37°C as compared with 0°C with these human WT1-specific TCR chains, the K_D could not be calculated at 37°C (Table I). Thus, in contrast to

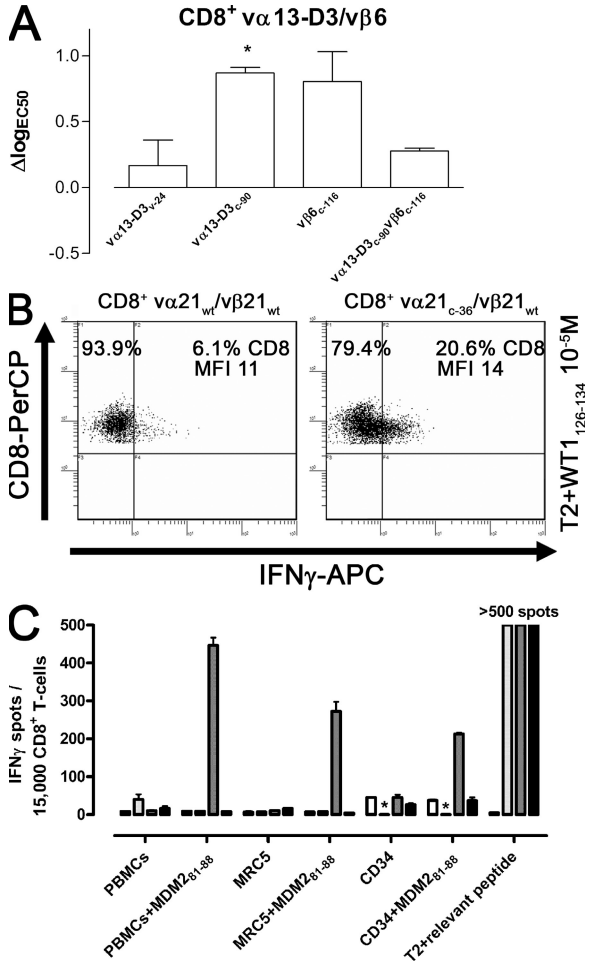

Figure 6. Analysis of T cells transduced with TCRs of other specificities. (A) $\Delta\log_{EC50}$ of WT and Δvα13-D3/vβ6 TCR–transduced CD8$^+$ T cells. Statistical significance was assessed by a *t* test (*, P < 0.05; error bars are SEM of at least two independent experiments). (B) Intracellular IFN-γ secretion of vα21$_{WT}$/vβ21$_{WT}$ and vα21$_{c\text{-}36}$/vβ21$_{WT}$ TCR–transduced CD8$^+$ T cells was determined after a 5-h coincubation with T2 cells pulsed with 10^{-5} M WT1$_{126\text{-}134}$ peptide. Data are representative of three independent experiments. (C) Mock (white), vα3$_{c\text{-}90}$/vβ3$_{WT}$ (light gray), vα13-D3$_{c\text{-}90}$/vβ6$_{WT}$ (dark gray), and vα21$_{c\text{-}36}$/vβ21$_{WT}$ (black) –transduced T cells (from the left to right per cell line) were coincubated with HLA-A2–positive PBMCs, the fibroblast cell line MRC5, and CD34$^+$ cells pulsed with no peptide or 10^{-6} M MDM2$_{81\text{-}88}$ as a positive control for the potential to be recognized by a specific T cell in this assay, and IFN-γ secretion was measured by an ELISPOT assay. T2 cells were pulsed with no peptide or the relevant peptide (10^{-6} M) for each TCR-transduced T cell (MDM2$_{81\text{-}88}$ for the mock-transduced T cells). Data are representative of two independent experiments. *, not done.

mouse TCR chains, removal of the *N*-glycosylation motif in the α chain at the interspecies conserved position c-90 did not improve functional avidity; however, depletion of the c-36 (Fig. 6 B) in the human α chain showed an almost 3.4-fold increase in cytokine-secreting cells, indicating that removal of *N*-glycosylation sites in a human TCR chain can also improve the avidity of TCR-transduced T cells.

Gain of functional avidity mediated by *N*-deglycosylated TCR chains does not result in self-reactivity

An undesirable effect of an increased avidity of a tumor antigen–specific T cell might be the recognition of normal tissue either by aberrant recognition of self-antigens (26) or recognition of the specifically targeted tumor antigen, such as WT1 (27), p53 (28), or MDM2 (3), because of the physiological expression of the protein at lower levels in normal tissues. To test whether the increased avidity provided by deglycosylation of the human $WT1_{126\text{-}134}$–, mouse $p53_{264\text{-}272}$–, or mouse $MDM2_{81\text{-}88}$–specific HLA-A2–restricted TCR chains results in aberrant recognition of normal tissue, $CD8^+$ T cells were mock transduced or transduced with the unmodified TCR β chain and the matched TCR α chains depleted for the *N*-glycosylation motif at position c-36 (human) or c-90 (mouse), and were coincubated with a panel of normal HLA-A2–positive cells (PBMCs, the fibroblast cell line MRC5, and $CD34^+$ cells). As a positive control for the ability of these targets to be recognized, the target cells were also evaluated after pulsing with $MDM2_{81\text{-}88}$ at 10^{-6} M. All of these cell lines have previously been demonstrated not to be recognized by T cells transduced with the WT TCR chains used in this study, and recognition of the potential partial HLA mismatch by endogenous TCRs has previously been shown not to read out in this assay (3, 4, 9, 21). As an additional positive control for the activity of TCR-transduced T cells, T2 cell targets were either not pulsed or pulsed with the relevant peptide (10^{-6} M). IFN-γ secretion was measured by ELISPOT, and the reactivity of mock- and ΔTCR-transduced T cells was compared. ΔTCR-transduced T cells, similar to mock-transduced T cells, failed to recognize normal tissue targets (Fig. 6 C), whereas these normal target cells pulsed with the MDM2 peptide induced IFN-γ secretion by T cells transduced with this ΔTCR, suggesting that the normal target cells could be recognized but that the gain of functional avidity mediated by the *N*-deglycosylated TCR chains does not result in acquisition of self-reactivity against this set of normal cells.

With the modified WT1-specific TCR, which was initially isolated from a normal human peripheral repertoire, it was also possible to analyze for potentially harmful in vivo reactivity with normal tissues in mice transgenic for human HLA-A2. The tissue distribution of expression of WT1 in normal tissues in mice is nearly identical to humans (29, 30), the sequence of the human epitope recognized by the human $WT1_{126\text{-}134}$–specific TCR is 100% identical in the mouse WT1 gene, the $WT1_{126\text{-}134}$ epitope has been shown to be efficiently processed and presented by mouse cells (31, 32), and transfer of $WT1_{126\text{-}134}$–specific TCR-transduced human T cells has been reported to induce therapeutic responses in nonobese diabetic (NOD)/severe combined immunodeficiency (SCID) mice without detectable xenoreactivity (5) with the mouse MHC molecules. This has allowed us to test if the physiological levels of $WT1_{126\text{-}134}$ in any tissue might be recognized by $WT1_{126\text{-}134}$–specific TCR-transduced human T cells in vivo by transferring the human T cells into NOD/SCID mice bred to express a transgenic HLA-A2 allele (HLA-A2 × NOD/SCID), as well as if aberrant reactivity with normal host proteins presented in the context of HLA-A2 is acquired by the modified TCR. 2×10^6 $vα21_{WT}/vβ21_{WT}$ and $vα21_{c\text{-}36}/vβ21_{WT}$ TCR–transduced human T cells were selected for equivalent TCR expression as described in earlier experiments, labeled with CFSE, and intravenously injected into HLA-A2 × NOD/SCID or NOD/SCID mice. HLA-A2 × NOD/SCID mice were simultaneously immunized to facilitate engraftment with 10 μg $WT1_{126\text{-}134}$ peptide or 10 μg of the control A/PR/8/34 influenza matrix protein M1 $FluM1_{58\text{-}66}$ (33). NOD/SCID mice were immunized only with 10 μg $WT1_{126\text{-}134}$ peptide. 6 h later, mice received a single subcutaneous injection of 6×10^5 IU of rhIL-2 resuspended in incomplete Freund's adjuvant (34) to enhance in vivo activation, survival, and expansion of the transferred cells. Mice were monitored for overall survival, weight loss, and persistence of the transferred transduced T cells. $CD8^+$ T cells transduced with WT and mutated TCR chains were detected by flow cytometry in the peripheral blood of HLA-A2 × NOD/SCID mice immunized with the$WT1_{126\text{-}134}$ peptide 2 wk after cell transfer ($n = 8$; mean $vα21_{WT}/vβ21_{WT}$, 1%; mean $vα21_{c\text{-}36}/vβ21_{WT}$, 1.3%), whereas <0.5% of T cells (below the detection threshold) were detectable at 2 wk in HLA-A2 × NOD/SCID mice immunized with $FluM1_{58\text{-}66}$ or NOD/SCID control mice immunized with the WT1 peptide but that lack the HLA-A2 allele on host cells required to present the peptide ($n = 16$), suggesting that antigen-specific proliferation of TCR-transduced T cells was induced by the peptide binding to recipient HLA-A2 in vivo (Fig. S4 A, available at http://www.jem.org/cgi/content/full/jem.20082487/DC1). In vivo proliferation of T cells after transfer and immunization was confirmed by analyzing the dilution of CFSE in the transferred $CD8^+$ T cells, which was not diluted on day 0 but became diluted after 2 wk in immunized mice expressing HLA-A2 (Fig. S4 B). HLA-A2 × NOD/SCID mice in which proliferation of T cells with WT and mutated TCR chains was observed did not show any clinical sign of autoimmunity after 2 wk and remained healthy through a 4-wk observation period, suggesting no significant toxicity mediated by the transferred T cells. After 4 wk, a time when transferred T cells could no longer be detected in the peripheral blood (unpublished data), the HLA-A2 × NOD/SCID mice were killed, organs (liver, spleen, and lung) were analyzed for histological signs of autoimmune injury, and bone marrow and spleen cells were analyzed by flow cytometry for the presence of $CD8^+$ T cells. No infiltrating human T cells were observed in the liver, lung, and bone marrow, and a normal histological structure of the liver, lung, and spleen

was observed. Transduced T cells were detected in the spleen of mice that received T cells with mutated TCR chains ($v\alpha21_{c\text{-}36}/v\beta21_{WT}$, 6.6%) but were below the detection threshold in recipients of T cells with WT TCR chains ($v\alpha21_{WT}/v\beta21_{WT}$, <0.5%; Fig. S4 C). Thus, the increased avidity of T cells transduced with the ΔTCR for targets presenting WT1 resulted in a greater initial expansion in response to in vivo immunization and improved long-term persistence without evidence of toxicity to normal tissues.

DISCUSSION

We observed enhanced functional avidity as reflected by cytokine secretion and lytic capacity after recognition of peptide-loaded targets, and improved recognition of tumor cells by T cells harboring ΔTCR. This was observed with both TCRs that exhibited a high affinity in their WT form (3, 4) and a TCR that initially exhibited a more intermediate affinity (9). Reducing *N*-glycosylation of TCRs might be directly enhancing the interaction of TCRs with pMHCs and thereby increasing T cell activation. Two models have been proposed to explain how TCR–pMHC interactions result in T cell activation (24, 35). The kinetic proofreading model proposes that the signaling machinery of T cells becomes activated once an activation threshold based on the time of occupancy of the TCR–CD3 cluster by the pMHC is reached, and the alternative model proposes that the agonist pMHC induces a specific conformational change in the TCR–CD3 that affects the quality of signals emanating from the ligated TCR–CD3 complex. In the former model, events such as TCR clustering/multimerization would be anticipated to contribute to the time of occupancy by increasing the number of concurrent interactions, and ΔTCR appendages might enhance T cell activation by facilitating TCR multimerization (24, 35). In the latter model, the requisite conformational changes might be more readily achieved in the context of reduced *N*-glycosylated appendages on the TCR chains.

Enhanced tetramer staining of ΔTCR- compared with WT TCR–transduced T cells was observed in our studies at 37°C but not 4°C, indicating that temperature-dependent mechanisms are involved in the improved TCR–pMHC interaction. More detailed analysis revealed that tetramer dissociation was significantly prolonged (up to approximately ninefold), whereas tetramer association was stable (36, 37). Thus, the observed improved binding of pMHC complexes and functional avidity of transduced cells was a consequence of the TCR complexes remaining associated for longer periods after binding had occurred rather than a result of binding more quickly. Structural analysis of *N*-linked oligosaccharide in the constant domain (Fig. 7) excluded that sugars linked to the constant TCR domains directly interact with a pMHC ligand. The slow off rate could therefore reflect either greater clustering/multimerization or the assumption of a conformation after pMHC interaction that binds more avidly, and either event would be expected to be temperature dependent. Moreover, directly enhanced signaling through complexes formed by ΔTCR as compared with WT TCR chains is also suggested by the rather small improvement in tetramer binding at 37°C that was associated with the more impressive improvement in function.

The CD8 complex was not required for mediating the phenotype observed in ΔTCR- as compared with WT TCR–transduced T cells, as indicated by the improved functional avidity detected in $CD4^+CD8^-$ T cells transduced with a TCR previously demonstrated to be capable of eliciting a CD8-independent signal (4). The lack of a requirement for CD8 is consistent with the structural analysis of the interaction site between CD8 and the TCR–pMHC, which is devoid of carbohydrates (38). Moreover, in cells expressing the CD8

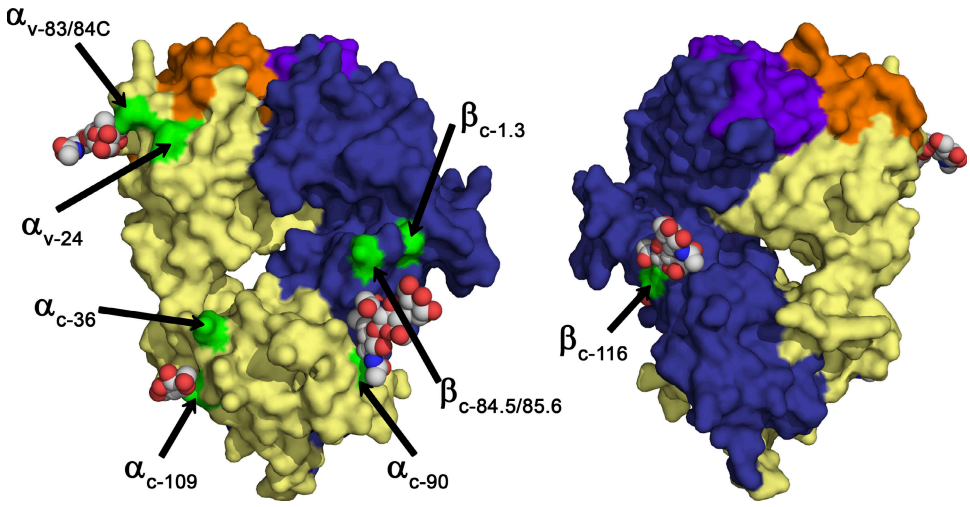

Figure 7. Molecular surface representation of the 2C TCR. Molecular surface representation of the 2C TCR (available from the Protein Data Bank under accession no. 1TCR; reference 52), colored by chain (α, yellow; β, blue) and CDR region (α-CDRs, orange; β-CDRs, purple), showing the location of asparagine residues at *N*-linked oligosaccharide sites (green). Two views are shown, rotated by 180° around the vertical axis. Ordered *N*-linked oligosaccharides are shown in the space-filling atom representation, colored by atom type (carbon, gray; nitrogen, blue; oxygen, red) when present in the 2C crystal structure.

coreceptor, the relative improvement in functional avidity as a result of expressing ΔTCR chains did not exceed the relative improvement in $CD4^+CD8^-$ T cells, suggesting that modified interactions of the deglycosylated TCR chain with CD8 were likely not playing a major role in the observed change in functional avidity. Although our analysis of mutated TCRs that are CD8 dependent (mouse, vα13-D3/vβ6; and human, vα21/vβ21) did not reveal that such TCRs become CD8 independent after transduction into $CD4^+$ T cells (unpublished data) despite evidence of improved avidity if expressed in $CD8^+$ T cells, this more likely reflected the magnitude of change to achieve CD8 independence with these TCRs rather than a dependence on interaction with CD8.

Multiple mechanisms have been proposed to influence the fine tuning of T cell responsiveness, including modulation of glycosylation of the CD8 molecule (18). Although regulation of *N*-glycosylation has been reported to affect T cell function (39, 40), and T cells in distinct differentiation states exhibit different levels of glycosylation (immature/mature and naive/memory) (15, 16), there has been no direct evidence that altered *N*-glycosylation of TCR chains is a physiological mechanism to tune reactivity via modulating avidity. For example, activation of naive T cells could result in reduced *N*-glycosylation of TCR chains that could contribute to the improved functional avidity observed in antigen-experienced T cells. Differentially *N*-glycosylated TCR complexes have also been observed in mature CD4 as compared with CD8 T cells (41), but the role of such differential *N*-glycosylation in defined T cell subsets has not yet been investigated.

In summary, we demonstrate that reduced *N*-glycosylation of TCR chains can improve functional avidity of TCR-transduced T cells in the absence and presence of the coreceptor CD8. We suggest that removal of specific *N*-glycosylation sites, in particular c-90 in the mouse TCR α chain, allows a temperature-dependent change, such as improved TCR multimerization resulting in a diminished TCR–pMHC dissociation and, therefore, more efficient T cell activation. Regardless of the individual mechanisms, this strategy can improve the avidity and potentially the efficacy of TCR-transduced T cells and may therefore prove useful for current efforts to redirect the immune system against cancer cells.

MATERIALS AND METHODS

Peptides, antibodies, multimeric complexes, and cytokines. Peptides $p53_{264\text{-}272}$, $MDM2_{81\text{-}88}$, and $WT1_{126\text{-}134}$, and the A/PR/8/34 influenza matrix protein M1 $FluM1_{58\text{-}66}$ were synthesized by SynPep. Anti–human–CD8–FITC/PerCP/PCY5 and anti–human–vβ21–FITC (Beckman Coulter), and anti-muβ/muvβ3/muvβ6TCR–PE/Pcy5 (BD) were commercially obtained. PE-labeled $p53_{264\text{-}272}$, $MDM2_{81\text{-}88}$, and $WT1_{126\text{-}134}$ tetramer HLA-A2 complexes were synthesized as previously described (42). Capture/detector antibody pairs for use in IL-2 and IFN-γ ELISA analysis were purchased from R&D Systems. IFN-γ ELISPOT was performed with 1D1K and 7B61 capture and detection antibodies (Mabtech). IL-2 was obtained from Chiron, and αCD3 (OKT3; Muromonab) was obtained from Ortho-Biotec.

Cell lines. The TCR-deficient cell line $58\alpha^-\beta^-$ was provided by B. Malissen (Centre d' Immunologie Marseille-Luminy, Marseille, France). The TAP-deficient HLA-A2–positive cell line T2, and the HLA-A2–positive p53 overexpressing cell lines MDAMB231 (breast cancer) and SW480 (colorectal cancer), were obtained from the American Type Culture Collection, and the cell line MZ1851RC (renal cell cancer) was obtained from B. Seliger (University of Halle, Halle, Germany). The HLA-A2–positive normal fibroblast cell line MRC5 was obtained from the American Type Culture Collection, and PBMCs and $CD34^+$ cells were isolated from leukaphereses of HLA-A2–positive healthy donors. The retroviral packaging cell line Phoenix-Ampho was obtained from the American Type Culture Collection. The HLA-A2–positive p53-negative tumor cell line Saos2 (osteosarcoma) was a gift of A. Levine (Princeton University, Princeton, NJ), and the K562-A2 (myeloblastic) cell line was provided by T. Wölfel (University of Mainz, Mainz, Germany).

WT and modified TCR chains, and TCR-transduced T cell lines. $p53_{264\text{-}272}$–specific (vα3/vβ3, mouse) (4), $MDM2_{81\text{-}88}$–specific (vα13-D3/vβ6, mouse) (3), and $WT1_{126\text{-}134}$–specific (vα21/vβ21, human) (9) TCR chains are described in Fig. 1 A. *N*-glycosylation-sites (N-X-S/T) of α and β TCR chains are indicated in Fig. 1 (B and C) and are depicted according to the international IMGT system (available at http://imgt.cines.fr/) (20). The prefix "v" was added if the *N*-glycosylation site was located in the variable domain, and the prefix "c" as added if it was located in the constant domain. To prevent *N*-glycosylation of TCR chains, the N in the *N*-glcyosylation site was changed to Q by site-directed mutagenesis (primers are shown in Table S1, available at http://www.jem.org/cgi/content/full/jem.20082487/DC1). Successful mutagenesis was confirmed by sequencing. This modification has been shown to prevent *N*-glycosylation of TCR chains (43). The $WT1_{126\text{-}134}$ TCRs have been further modified by introducing point mutations in the constant domains of both chains, as previously described to insert cysteines that can form a disulfide bond and improve matched pairing and surface expression (9). T cell transduction with modified and WT TCR chains was performed as previously described (44). In brief, Phoenix-Ampho cells were transfected using a transfection reagent (Fugene; Takara) with vectors containing the TCR chain (pBullet), gag-pol (pHIT60), and env (pCOLT-GALV) (3). Human PBMCs activated with 30ng/ml αCD3 were transduced twice within 48 h in the presence of 40–100 IU/ml IL-2 and 4 μg/ml polybrene (Sigma-Aldrich), with a packaging cell supernatant containing retroviral vectors encoding for no protein (empty cassette), GFP (control), or α or β TCR chains. Downstream of the coding regions, IRES-puro (coding region: empty cassette or α chain) and -neo (coding region: empty cassette, GFP, or β chain; BD) cassettes were attached, respectively. Transduced T cells were expanded by weekly stimulation with αCD3/CD28 Dynabeads (1 μl per 10^6 cells; Invitrogen) and 40–100 IU/ml rhIL-2, and were selected with 800 μg/ml geneticin (Invitrogen) and 5 μg/ml puromycin (Sigma-Aldrich) for 1 wk. Polyclonal $CD4^+$ and $CD8^+$ T cells transduced with α and β chains were sorted based on CD4 or CD8 expression and the level of TCR β chain surface expression and were expanded in vitro using the rapid expansion protocol, as previously described (45).

RT-PCR, flow-cytometry, and T cell assays. Expression of introduced α and β TCR chain was quantified by flow cytometry using antibodies with specificity for the β chain, or by real-time PCR (TaqMan; Applied Biosystems) by using primers specific for the unique CDR3 region of the α and β chains. Standard ^{51}Cr-release (46), intracellular cytokine staining (47), ELISA (48), and IFN-γ ELISPOT assays (33) were performed as previously described. To assess the functional avidity of TCR-transduced cells, the EC50 (the concentration of peptide needed for half maximal cytokine secretion) was calculated and transformed to $\log_{EC50} \pm$ SEM. To normalize gain of functional avidity for cells with Δ as compared with WT TCR chains, "log change in functional avidity" ($\Delta\log_{EC50}$) was calculated by subtracting $\log_{EC50}$ from cells transduced with ΔTCR chains, from $\log_{EC50}$ of cells transduced with WT TCR chains. To assess avidity (K_D) for TCR–pMHC binding, TCR-transduced cells were incubated with varying concentrations of tetramer for 45 min to achieve equilibrium. MFI of tetramer binding was determined by flow cytometry and plotted against the concentration of tetramer used for staining. The avidity (K_D) was derived from the slope by

$K_D = -1/\text{slope}$ (Scatchard plot) (49, 50). To assess tetramer association (k_{on}) and dissociation (k_{off}), TCR-transduced cells were incubated with tetramer for 45 min. K_{ob}, the value of K determined by fitting an exponential association equation to the data, was determined. Then, the excess of HLA class I blocking antibody (1 mg/ml; W6/32 [Abcam] or supernatant from the cell line HB-95 [American Type Culture Collection]) (51) or no blocking antibody was added, and the MFI of tetramer binding after 2, 5, 10, 15, 20, 40, and 60 min was again determined. Only in the presence of the blocking antibody W6/32 was a decrease in the MFI of tetramer binding observed. Furthermore, the number of TCR complexes, as assessed by a vβ-specific monoclonal antibody before and after incubation at 37°C, were identical in WT- and ΔTCR-transduced T cells, suggesting no difference in endocytosis of TCR complexes during the time of the dissociation experiment. The times needed for half-maximal inhibition of tetramer binding ($t_{1/2}$) and K_{off}, the dissociation rate constant, were determined. Then, k_{on} and K_D were calculated ($k_{on} = (k_{ob} - k_{off})$/ligand concentration; $K_D = k_{off}/k_{on}$).

Adoptive T cell transfer. NOD/SCID mice were bred to express a transgenic HLA-A2 allele (HLA-A2 × NOD/SCID). Irradiated (150 rad) NOD/SCID or HLA-A2 × NOD/SCID mice were intravenously injected with 2×10^6 human $v\alpha21_{WT}/v\beta21_{WT}$ and $v\alpha21_{c\text{-}36}/v\beta21_{WT}$ TCR–transduced T cells selected for equivalent TCR expression, as described in earlier experiments, labeled with CFSE. The HLA-A2 × NOD/SCID and NOD/SCID mice were then immediately immunized subcutaneously once with 10 μg $WT1_{126\text{-}134}$ peptide or the A/PR/8/34 influenza matrix protein $FluM1_{58\text{-}66}$ (33), as indicated in the figures, and this was followed 6 h later by a single subcutaneous injection of 6×10^5 IU rhIL-2 resuspended in incomplete Freund's adjuvant. Peripheral blood was obtained by tail bleeding after 2 and 4 wk. Mice were propagated and maintained at the Johannes Gutenberg University. Animal experiments were approved by the local authorities (Landesuntersuchungsamt Rheinland Pfalz, Dienststelle Tierschutz, Mainz, Germany). All experimental procedures were performed according to the National Institutes of Health Guide for the Care and Use of Laboratory Animals.

Online supplemental material. Fig. S1 shows TCR β chain staining of ΔTCR-transduced $58\alpha^-\beta^-$ hybridoma cells, Fig. S2 shows tetramer staining of ΔTCR-transduced $58\alpha^-\beta^-$ hybridoma cells, and Fig. S3 shows TCR internalization after antigen encounter. Fig. S4 shows antigen-specific in vivo proliferation of TCR-transduced T cells. Table S1 shows primers used for site-directed mutagenesis. Online supplemental material is available at http://www.jem.org/cgi/content/full/jem.20082487/DC1.

We are grateful to J. Cao, H.N. Nguyen, M. Brkic, Dr. M. Jülch, M. Grabowski, Dr. A. Kreft, and L. Hartkamp for expert technical contributions.

This work was supported by grants from the Leukemia and Lymphoma Society (LLS 7040-03), the National Institutes of Health (P01 CA18029 and R37 CA33084), the Deutsche Forschungsgemeinschaft (SFB 432 A3), the European Commission, the ZonMW (40-40300-98-07003), and the Wilhelm-Laupitz Foundation. J. Kuball and M. Wolfl have been fellows of the Deutsche Krebshilfe.

The authors have no conflicting financial interests.

Submitted: 3 November 2008
Accepted: 30 December 2008

REFERENCES

1. Schumacher, T.N. 2002. T-cell-receptor gene therapy. *Nat. Rev. Immunol.* 2:512–519.
2. Morgan, R.A., M.E. Dudley, J.R. Wunderlich, M.S. Hughes, J.C. Yang, R.M. Sherry, R.E. Royal, S.L. Topalian, U.S. Kammula, N.P. Restifo, et al. 2006. Cancer regression in patients after transfer of genetically engineered lymphocytes. *Science.* 314:126–129.
3. Stanislawski, T., R.H. Voss, C. Lotz, E. Sadovnikova, R.A. Willemsen, J. Kuball, T. Ruppert, R.L. Bolhuis, C.J. Melief, C. Huber, et al. 2001. Circumventing tolerance to a human MDM2-derived tumor antigen by TCR gene transfer. *Nat. Immunol.* 2:962–970.
4. Kuball, J., F.W. Schmitz, R.H. Voss, E.A. Ferreira, R. Engel, P. Guillaume, S. Strand, P. Romero, C. Huber, L.A. Sherman, and M. Theobald. 2005. Cooperation of human tumor-reactive CD4(+) and CD8(+) T cells after redirection of their specificity by a high-affinity p53A2.1-specific TCR. *Immunity.* 22:117–129.
5. Xue, S.A., L. Gao, D. Hart, R. Gillmore, W. Qasim, A. Thrasher, J. Apperley, B. Engels, W. Uckert, E. Morris, and H. Stauss. 2005. Elimination of human leukemia cells in NOD/SCID mice by WT1-TCR gene-transduced human T cells. *Blood.* 106:3062–3067.
6. Holler, P.D., P.O. Holman, E.V. Shusta, S. O'Herrin, K.D. Wittrup, and D.M. Kranz. 2000. In vitro evolution of a T cell receptor with high affinity for peptide/MHC. *Proc. Natl. Acad. Sci. USA.* 97:5387–5392.
7. Li, Y., R. Moysey, P.E. Molloy, A.L. Vuidepot, T. Mahon, E. Baston, S. Dunn, N. Liddy, J. Jacob, B.K. Jakobsen, and J.M. Boulter. 2005. Directed evolution of human T-cell receptors with picomolar affinities by phage display. *Nat. Biotechnol.* 23:349–354.
8. Cohen, C.J., Y. Zhao, Z. Zheng, S.A. Rosenberg, and R.A. Morgan. 2006. Enhanced antitumor activity of murine-human hybrid T-cell receptor (TCR) in human lymphocytes is associated with improved pairing and TCR/CD3 stability. *Cancer Res.* 66:8878–8886.
9. Kuball, J., M.L. Dossett, M. Wolfl, W.Y. Ho, R.H. Voss, C. Fowler, and P.D. Greenberg. 2007. Facilitating matched pairing and expression of TCR chains introduced into human T cells. *Blood.* 109:2331–2338.
10. Daniels, M.A., K.A. Hogquist, and S.C. Jameson. 2002. Sweet 'n' sour: the impact of differential glycosylation on T cell responses. *Nat. Immunol.* 3:903–910.
11. Lowe, J.B. 2001. Glycosylation, immunity, and autoimmunity. *Cell.* 104:809–812.
12. Brennan, P.J., S.J. Saouaf, S. Van Dyken, J.D. Marth, B. Li, A. Bhandoola, and M.I. Greene. 2006. Sialylation regulates peripheral tolerance in CD4+ T cells. *Int. Immunol.* 18:627–635.
13. Garcia, G.G., and R.A. Miller. 2003. Age-related defects in CD4+ T cell activation reversed by glycoprotein endopeptidase. *Eur. J. Immunol.* 33:3464–3472.
14. Garcia, G.G., S.B. Berger, A.A. Sadighi Akha, and R.A. Miller. 2005. Age-associated changes in glycosylation of CD43 and CD45 on mouse CD4 T cells. *Eur. J. Immunol.* 35:622–631.
15. Galvan, M., K. Murali-Krishna, L.L. Ming, L. Baum, and R. Ahmed. 1998. Alterations in cell surface carbohydrates on T cells from virally infected mice can distinguish effector/memory CD8+ T cells from naive cells. *J. Immunol.* 161:641–648.
16. Pappu, B.P., and P.A. Shrikant. 2004. Alteration of cell surface sialylation regulates antigen-induced naive CD8+ T cell responses. *J. Immunol.* 173:275–284.
17. Moody, A.M., D. Chui, P.A. Reche, J.J. Priatel, J.D. Marth, and E.L. Reinherz. 2001. Developmentally regulated glycosylation of the CD8alphabeta coreceptor stalk modulates ligand binding. *Cell.* 107:501–512.
18. Daniels, M.A., L. Devine, J.D. Miller, J.M. Moser, A.E. Lukacher, J.D. Altman, P. Kavathas, K.A. Hogquist, and S.C. Jameson. 2001. CD8 binding to MHC class I molecules is influenced by T cell maturation and glycosylation. *Immunity.* 15:1051–1061.
19. Demetriou, M., M. Granovsky, S. Quaggin, and J.W. Dennis. 2001. Negative regulation of T-cell activation and autoimmunity by Mgat5 N- glycosylation. *Nature.* 409:733–739.
20. Lefranc, M.P. 2003. IMGT, the international ImMunoGeneTics database. *Nucleic Acids Res.* 31:307–310.
21. Voss, R.H., J. Kuball, R. Engel, P. Guillaume, P. Romero, C. Huber, and M. Theobald. 2006. Redirection of T cells by delivering a transgenic mouse-derived MDM2 tumor antigen-specific TCR and its humanized derivative is governed by the CD8 coreceptor and affects natural human TCR expression. *Immunol. Res.* 34:67–87.
22. Sommermeyer, D., J. Neudorfer, M. Weinhold, M. Leisegang, B. Engels, E. Noessner, M.H. Heemskerk, J. Charo, D.J. Schendel, T. Blankenstein, et al. 2006. Designer T cells by T cell receptor replacement. *Eur. J. Immunol.* 36:3052–3059.
23. Whelan, J.A., P.R. Dunbar, D.A. Price, M.A. Purbhoo, F. Lechner, G.S. Ogg, G. Griffiths, R.E. Phillips, V. Cerundolo, and A.K. Sewell. 1999.

Specificity of CTL interactions with peptide-MHC class I tetrameric complexes is temperature dependent. *J. Immunol.* 163:4342–4348.
24. Alam, S.M., G.M. Davies, C.M. Lin, T. Zal, W. Nasholds, S.C. Jameson, K.A. Hogquist, N.R. Gascoigne, and P.J. Travers. 1999. Qualitative and quantitative differences in T cell receptor binding of agonist and antagonist ligands. *Immunity*. 10:227–237.
25. Willcox, B.E., G.F. Gao, J.R. Wyer, J.E. Ladbury, J.I. Bell, B.K. Jakobsen, and P.A. van der Merwe. 1999. TCR binding to peptide-MHC stabilizes a flexible recognition interface. *Immunity*. 10:357–365.
26. Holler, P.D., L.K. Chlewicki, and D.M. Kranz. 2003. TCRs with high affinity for foreign pMHC show self-reactivity. *Nat. Immunol.* 4:55–62.
27. Gao, L., I. Bellantuono, A. Elsasser, S.B. Marley, M.Y. Gordon, J.M. Goldman, and H.J. Stauss. 2000. Selective elimination of leukemic CD34(+) progenitor cells by cytotoxic T lymphocytes specific for WT1. *Blood.* 95:2198–2203.
28. Theobald, M., J. Biggs, J. Hernandez, J. Lustgarten, C. Labadie, and L.A. Sherman. 1997. Tolerance to p53 by A2.1-restricted cytotoxic T lymphocytes. *J. Exp. Med.* 185:833–841.
29. Buckler, A.J., J. Pelletier, D.A. Haber, T. Glaser, and D.E. Housman. 1991. Isolation, characterization, and expression of the murine Wilms' tumor gene (WT1) during kidney development. *Mol. Cell. Biol.* 11:1707–1712.
30. Fraizer, G.C., P. Patmasiriwat, X. Zhang, and G.F. Saunders. 1995. Expression of the tumor suppressor gene WT1 in both human and mouse bone marrow. *Blood.* 86:4704–4706.
31. Gaiger, A., V. Reese, M.L. Disis, and M.A. Cheever. 2000. Immunity to WT1 in the animal model and in patients with acute myeloid leukemia. *Blood.* 96:1480–1489.
32. Tsuboi, A., Y. Oka, H. Ogawa, O.A. Elisseeva, H. Li, K. Kawasaki, K. Aozasa, T. Kishimoto, K. Udaka, and H. Sugiyama. 2000. Cytotoxic T-lymphocyte responses elicited to Wilms' tumor gene WT1 product by DNA vaccination. *J. Clin. Immunol.* 20:195–202.
33. Kuball, J., M. Schuler, F.E. Antunes, W. Herr, M. Neumann, L. Obenauer-Kutner, L. Westreich, C. Huber, T. Wolfel, and M. Theobald. 2002. Generating p53-specific cytotoxic T lymphocytes by recombinant adenoviral vector-based vaccination in mice, but not man. *Gene Ther.* 9:833–843.
34. Huber, C., N. Bobek, J. Kuball, S. Thaler, S. Hoffarth, C. Huber, M. Theobald, and M. Schuler. 2005. Inhibitors of apoptosis confer resistance to tumour suppression by adoptively transplanted cytotoxic T-lymphocytes in vitro and in vivo. *Cell Death Differ.* 12:317–325.
35. Schamel, W.W., I. Arechaga, R.M. Risueno, H.M. van Santen, P. Cabezas, C. Risco, J.M. Valpuesta, and B. Alarcon. 2005. Coexistence of multivalent and monovalent TCRs explains high sensitivity and wide range of response. *J. Exp. Med.* 202:493–503.
36. Alam, S.M., P.J. Travers, J.L. Wung, W. Nasholds, S. Redpath, S.C. Jameson, and N.R. Gascoigne. 1996. T-cell-receptor affinity and thymocyte positive selection. *Nature.* 381:616–620.
37. Lyons, D.S., S.A. Lieberman, J. Hampl, J.J. Boniface, Y. Chien, L.J. Berg, and M.M. Davis. 1996. A TCR binds to antagonist ligands with lower affinities and faster dissociation rates than to agonists. *Immunity*. 5:53–61.
38. Rudd, P.M., M.R. Wormald, R.L. Stanfield, M. Huang, N. Mattsson, J.A. Speir, J.A. DiGennaro, J.S. Fetrow, R.A. Dwek, and I.A. Wilson. 1999. Roles for glycosylation of cell surface receptors involved in cellular immune recognition. *J. Mol. Biol.* 293:351–366.
39. Lau, K.S., E.A. Partridge, A. Grigorian, C.I. Silvescu, V.N. Reinhold, M. Demetriou, and J.W. Dennis. 2007. Complex N-glycan number and degree of branching cooperate to regulate cell proliferation and differentiation. *Cell.* 129:123–134.
40. Grigorian, A., S.U. Lee, W. Tian, I.J. Chen, G. Gao, R. Mendelsohn, J.W. Dennis, and M. Demetriou. 2007. Control of T cell-mediated autoimmunity by metabolite flux to N-glycan biosynthesis. *J. Biol. Chem.* 282:20027–20035.
41. Zapata, D.A., W.W. Schamel, P.S. Torres, B. Alarcon, N.E. Rossi, M.N. Navarro, M.L. Toribio, and J.R. Regueiro. 2004. Biochemical differences in the alphabeta T cell receptor.CD3 surface complex between CD8+ and CD4+ human mature T lymphocytes. *J. Biol. Chem.* 279:24485–24492.
42. Altman, J.D., P.A. Moss, P.J. Goulder, D.H. Barouch, M.G. McHeyzer-Williams, J.I. Bell, A.J. McMichael, and M.M. Davis. 1996. Phenotypic analysis of antigen-specific T lymphocytes. *Science.* 274:94–96.
43. Strong, R.K., D.M. Penny, R.M. Feldman, L.P. Weiner, J.J. Boniface, M.M. Davis, and P.J. Bjorkman. 1994. Engineering and expression of a secreted murine TCR with reduced N-linked glycosylation. *J. Immunol.* 153:4111–4121.
44. Voss, R.H., J. Kuball, and M. Theobald. 2005. Designing TCR for cancer immunotherapy. *Methods Mol. Med.* 109:229–256.
45. Riddell, S.R., and P.D. Greenberg. 1990. The use of anti-CD3 and anti-CD28 monoclonal antibodies to clone and expand human antigen-specific T cells. *J. Immunol. Methods.* 128:189–201.
46. Sherman, L.A., S.V. Hesse, M.J. Irwin, D. La Face, and P. Peterson. 1992. Selecting T cell receptors with high affinity for self-MHC by decreasing the contribution of CD8. *Science.* 258:815–818.
47. Ochsenbein, A.F., S.R. Riddell, M. Brown, L. Corey, G.M. Baerlocher, P.M. Lansdorp, and P.D. Greenberg. 2004. CD27 expression promotes long-term survival of functional effector-memory $CD8^+$ cytotoxic T lymphocytes in HIV-infected patients. *J. Exp. Med.* 200:1407–1417.
48. Blank, C., J. Kuball, S. Voelkl, H. Wiendl, B. Becker, B. Walter, O. Majdic, T.F. Gajewski, M. Theobald, R. Andreesen, and A. Mackensen. 2006. Blockade of PD-L1 (B7-H1) augments human tumor-specific T cell responses in vitro. *Int. J. Cancer.* 119:317–327.
49. Holmberg, K., S. Mariathasan, T. Ohteki, P.S. Ohashi, and N.R. Gascoigne. 2003. TCR binding kinetics measured with MHC class I tetramers reveal a positive selecting peptide with relatively high affinity for TCR. *J. Immunol.* 171:2427–2434.
50. Savage, P.A., J.J. Boniface, and M.M. Davis. 1999. A kinetic basis for T cell receptor repertoire selection during an immune response. *Immunity*. 10:485–492.
51. Konopitzky, R., U. Konig, R.G. Meyer, W. Sommergruber, T. Wolfel, and T. Schweighoffer. 2002. Identification of HLA-A*0201-restricted T cell epitopes derived from the novel overexpressed tumor antigen calcium-activated chloride channel 2. *J. Immunol.* 169:540–547.
52. Garcia, K.C., M. Degano, R.L. Stanfield, A. Brunmark, M.R. Jackson, P.A. Peterson, L. Teyton, and I.A. Wilson. 1996. An alphabeta T cell receptor structure at 2.5 A and its orientation in the TCR-MHC complex. *Science.* 274:209–219.